Received: 22 May 2019 | Revised: 24 October 2019 | Accepted: 25 October 2019
DOI: 10.1002/fam.2789

INTERFLAM 2019: HUMAN BEHAVIOR IN FIRE

WILEY

The influence of individual impairments in crowd dynamics

Paul Geoerg[1] | Jette Schumann[1] | Stefan Holl[2] | Maik Boltes[2] | Anja Hofmann[2]

[1]Bundesanstalt für Materialforschung und -prüfung, 7.5 Technical Properties of Polymeric Materials, Berlin, Germany
[2]Forschungszentrum Jülich GmbH, Civil Safety Research (IAS-7), Jülich, Germany

Correspondence
Paul Geoerg, 7.5 Technical Properties of Polymeric Materials, Bundesanstalt für Materialforschung und -prüfung, Berlin, Germany
Email: paul.geoerg@bam.de

Funding information
German Federal Ministry of Education and Research, Grant/Award Number: 13N13946 and 13N13950

Summary

The importance of empirical relations to quantify the movement of pedestrians through a facility has increased during the last decades since performance-based design methods became more common. Bottlenecks are of special interest because of their importance for egress routes and as they result in a reduced capacity. The empirical relations as the density-dependent movement speed or flow rate were derived by studies under laboratory conditions, which were usually conducted with populations of homogeneous characteristics for better control of influencing variables. If individual characteristics of a crowd become more heterogeneous, individuals were forced to adapt their individual movement and control individual manoeuvring. These unintended interactions lead to a different shape of the fundamental empirical relations. Here, we present results from a movement study under well-controlled boundary conditions in which participants with and without different characteristics of disabilities participated. To consider the effect of different heterogeneities on the capacity of a facility, fundamental diagrams are generated using the Voronoi method. If participants with visible disabilities (such as using assistive devices) are part of a crowd, significant differences relating to the shape of the empirical relations and the capacities are found. This indicates that the heterogeneity of a population leads to an increased interpersonal interaction which results in influenced movement characteristics.

KEYWORDS
engineering egress data, heterogeneity, human behaviour, movement characteristics, pedestrian dynamics

1 | INTRODUCTION

Pedestrian dynamics are important for consideration in any fire safety engineering design. Current regulations referenced on datasets, which are typically based on uniform (homogeneous) population settings, that have been published in the last decades.[1,2] At the same time, enormous efforts have been made to clarify the fundamentals of pedestrian movement during the last decades. The need for work in interdisciplinary teams on issues[3] is increasingly being used to focus several point of views (eg, previous studies[4,5]).

Gwynne and Boyce published a comprehensive overview on data for engineering quantification of egress.[6] In order to improve the understanding of the context of the data[7] a comprehensive focus was put on documentation of boundary conditions of the data sets. Data collection considering different levels of movement complexity was discussed by Shi et al.[8] Boltes et al[9] presented an extended overview of results of pedestrian and evacuation dynamics, and Haghani et al compiled a detailed discussion on empirical methods on crowd behaviour and motion.[10] Zou et al[11] had identified relevant research institutions for pedestrian dynamics by analysing bibliographic background information and publication details.

These structuring reviewing publications take particularly data of well-abled participants into account. Due to the recognition of three important mega-trends—mobility, urbanisation, and silver societies (demographic changes)—the use of these data based on homogeneous populations may lead to inapplicable functional relationship, nontransferable performance values, and loss of confidence in performance-based design principles. In particular, the results of the demographic transformation process (eg, increasing proportions of elderly or impaired persons) are not considered in functional relationships of movement and may have an effect on the assessment of crowd movement and evaluation of safe egress.[12]

However, few studies have considered truly heterogeneous groups or disabled pedestrians as evidenced by the small proportion of datasets presented in Gwynne and Boyce.[6] Geoerg et al had recently published an extended update on engineering egress data considering pedestrians with disabilites.[13] Findings regarding to unimpeded movement speed and empirical relations were discussed. Hashemi et al had published a survey of drill, simulations, and accesibility and provided data on different movement parameters and disabilities.[14]

The impact of a reduced visibility or vision loss on movement characteristics were investigated by previous studies.[15-20] In general, reduced flow rates and strongly effected movement speed of the individuals are reported. The influencing aspect of individuals using assistive devices (eg, wheelchairs) during crowd movement has been adressed by previous works.[21-23] Differences in individual movement speeds between wheelchair users and nondisabled participants were reported. A dependency between the ratio of wheelchair users in a population and the width of an opening was observed. Differences in empirical relations for elderly (or younger respectively) populations were reported by previous works.[24-33] Especially, reduced movement speed and flow rate were highlighted.

While an increased prevalence to die during a disaster for citizens with disability is well reported (eg, previous studies,[34-40] pp. 74-76[41]), it is debatable whether those data are still representative in terms of transferability to diverse, inhomogeneous, and more realistic populations.[1] This publication addresses this challenge and presents findings from well-controlled large-scale parameter studies on pedestrians movement through a bottleneck. Populations defined by different disabilities were considered. In contrast to a recently published study of the authors,[42] results of four different populations were compared: participants using wheelchairs (whe), with walking disabilities (wal), with mixed single disabilities (mix), and without any disabilities (ref).

The structure is organised as follows: in Section 2, the setting of the movement studies, the data extraction techniques, and the used calculation methods are introduced. The data analysis follows in Section 3. First, we present a comparison of unimpeded (unrestricted, free) movement speed (v_0) of different subpopulations (Section 3.1). Second, the impact of three subpopulations characterised by presence of participants with different types of impairments (participants using a wheelchair, participants with walking disabilities, and participants with mixed disabilities) on stability of movement in a group is discussed (Section 3.2). Especially, the effect on fundamental relationships $\bar{v}(\bar{\rho})$ and $\bar{J}(\bar{\rho}) = \bar{\rho} \cdot \bar{v}$ is examined in more detail (Section 4). The conclusion is made in the last section (Section 5).

2 | METHODOLOGY

2.1 | Study setup

The movement studies were conducted as a part of the interdisciplinary research project SiME. SiME is an acronym for the German meaning of "Safety for people with body-, mental- or age-related disabilities" and funded by the German Ministry of Education and Research (BMBF). Twelve studies with more than 145 single runs and overall 252 participants with and without disabilities were performed in an industrial hall in Wermelskirchen-Dabringhausen (Germany) in June 2017.

Participants without disabilities (NDP) were recruited by public call while participants with disabilities (PWD) were recruited from a sheltered workshop. For defining the type of disability and to consider and select participants with disabilities, we used a Score Regarding the Need for Assistance approach (Score RNA), which is a method to weight potentially critical indicators for egress (for details we refer to previous studies[43,44]). The Score RNA considers disabilities in reception (blindness, deafness), perception (cognition), and ability of movement (walking impairments, requirement on assistance devices), and in addition, a cross-section variable (age). This Score RNA evaluates

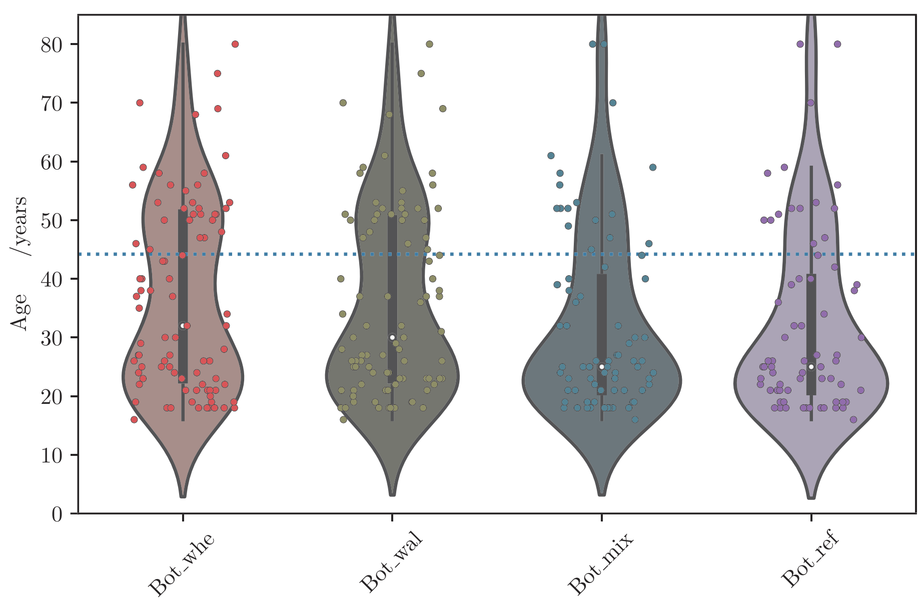

FIGURE 1 Age distribution of the participants in each study. For comparison, the average median age (44.4 years) for Germany in 2015 is plotted by the blue dotted line.[45] Overall, 48.5% of the participants were males. Please note that the x-position of the scattered data is just to present all data values [Colour figure can be viewed at wileyonlinelibrary.com]

the influence of the individual ability to evacuate autonomously. Here we present the influence on movement through a bottleneck (Figure 1) by absence and presence of subpopulations considering wheelchair users (Bot_whe), walking disabled (Bot_wal) and multiple severe-disabled participants (Bot_mix). This configuration follows the concept of increasing complexity of individual characteristics: first, a subpopulation of walking disabled represents the simplest case of complexity because the movement pattern is quite similar to the reference population. A more complex situation because of static space requirements (wheelchairs) does follow. These subpopulations are therefore a necessary simplification for the design of a persona "participants with single disability." For details of applying a persona, we kindly refer to Cao et al.[31] Afterwards, a subpopulation of multiple severe-disabled participants (considering blind, deaf, and wheelchair users) was analysed. In addition, all studies were repeated without a subpopulation with disabilities (reference studies – Bot_ref).

In accordance to the reported 10% of inhabitants that have disabilities in Germany[46] and the estimated prevalence of high and medium disabilities world wide is 15%,[47] a similar population was configured. This is in accordance to the prevalence of disability (approximately 15% for EU-27[48] and 19% for the United States[49]). The mean age of the disabled participants was 47.6 ± 7.0 years, the mean age of non-disabled participants was 35.9 ± 16.3. Detailed information of the age distribution of each study is presented in Figure 1. The mean age of the reference population was 32.1 ± 15.2. The body heights of all participants range from 1.45 to 2.04 m with a mean of 1.74 ± 0.1*m*.

Participation was absolutely voluntary for everybody and a cancellation of participation without any negative consequences was possible at any time. All participants have been paid €25 per half a day of participation. Only anonymous data were used for the studies and the methodological design, data storage process, and the access authorisation for data was approved by the ethics committee of the Bergische Universität Wuppertal. No ethical concerns were mentioned.

The aim of the studies was to investigate the impact of a heterogeneous characterised crowd (nondisabled participants and disabled participants) on performance criteria for movement in built environments under well-controlled conditions.

The geometry consists of two corridors of different widths. The rear, narrower part was varied *w* (see Figure 2) was varied in increments of 0.1m from 0.9 to 1.2m (Table 1). The front part was 2.4 m wider than the rear part and was used to canalise the direction of crowd movement. The initial density was about 3.0m^{-2}, and each configuration was repeated twice (see Table 1). In addition, every participant was walking through the geometry alone at the beginning (Run 00). The length of the bottleneck was here set constant with a length of 2.4 m.

The geometry was built from wooden three-layer panels with a height of 2.0 m. To buffer starting conditions and minimise the effect of the entrance, a waiting zone of approximately 30 m^2 was located at a distance of 15.0 m in front of the bottleneck entrance.

The participants were advised to move through the bottleneck without haste. It was emphasised not to push and to walk with the preferred movement speed. A trial was started by instructions of the experiment leader. When a participant leaves the geometry, he or she returns to the waiting zone for the next run. The performance criteria were measured in a measurement area of 4.0m^2 located 4.0 m in front of the bottleneck entrance (see Figures 2-6).

2.2 | Data extraction method

The movement through the study setting was captured by nine high-resolution cameras attached to the ceiling of the hall. Each participant wore a coloured cap according to their individual body height. We used the PeTrack-Framework to determine the automatic extraction of positions at every time step (frame) from the video recordings[50] PeTrack detects the centre of the coloured cap and tracks the position for the following time steps. For details of the method, we refer to Boltes et al[51] and applied to the presented study to Geoerg et al.[42] Figure 3 displays, for instance, the trajectories corresponding to a bottleneck configuration with a passage width of 1.2 m for each of the listed configuration of Tablereftab:rundetails. See Table 1 for details of the trial 08 indicated by the two-digit number. Participants with disabilities (Figure 3A: participants using a wheelchair, Figure 3B: participants with walking disabilities, Figure 3C: participants with mixed (single) disabilities, and Figure 3D: without participants with disabilities). A more detailed description on the individual characteristics of the participants with disabilities is provided in Geoerg et al.[52]

The maximum error e_{max} of the trajectories resulting from the perspective camera view is approximately 0.092 m for the camera

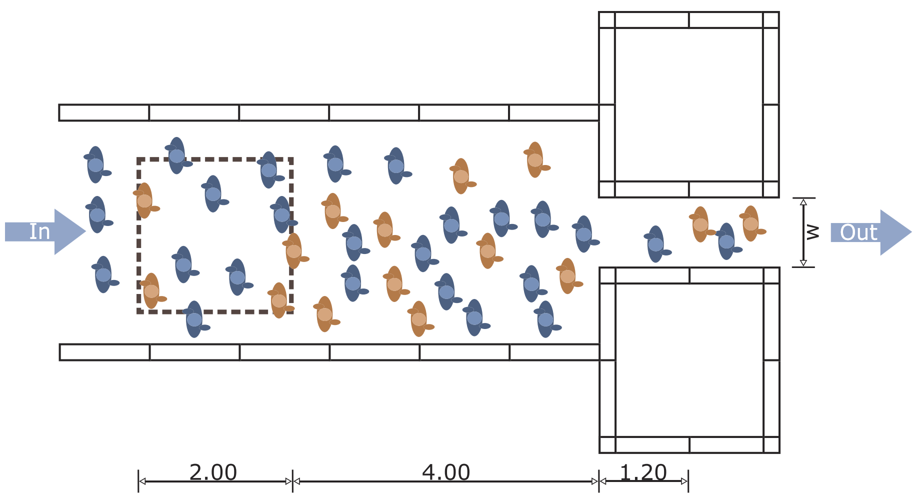

FIGURE 2 Sketch of the study setup. The width *w* was varied between 0.9 m and 1.2 m in steps of 0.1 m. Black rectangle: measurement area [Colour figure can be viewed at wileyonlinelibrary.com]

TABLE 1 Controlled boundary conditions and characteristics of each run

Bot_whe	Run	00	01	02	03	04	05	06	07	08
	w /m	0.9	0.9	0.9	1.0	1.0	1.1	1.1	1.2	1.2
	N (NDP)	70	81	81	80	80	83	83	85	83
	N (PWD)	7	7	7	7	7	7	1.1	1.2	7
Bot_wal	Run	00	01	02	03	04	05	06	07	08
	w /m	0.9	0.9	0.9	1.0	1.0	1.1	1.1	1.2	1.2
	N (NDP)	70	79	80	80	80	79	80	81	81
	N (PWD)	5	5	5	5	5	5	5	5	5
Bot_mix	Run	00	01	02	03	04	05	06	07	08
	w /m	0.9	0.9	0.9	1.0	1.0	1.1	1.1	1.2	1.2
	N (NDP)	74	75	74	74	75	75	75	75	75
	N (PWD)	5	5	5	5	5	5	5	5	5
Bot_ref	Run	00	01	02	03	04	05	06	07	08
	w /m	0.9	0.9	0.9	1.0	1.0	1.1	1.1	1.2	1.2
	N (NDP)	68	67	67	66	66	69	69	69	69
	N (PWD)	–	–	–	–	–	–	–	–	–

Note. Some participants have to rest after a run due to their disability and that volunteers without tasks participated run-wise. Abbreviations: Bot_mix, participants with different single disabilities; Bot_ref, all participants without disabilities; Bot_wal, participants with walking disabilities; Bot_whe, participants using a wheelchair; N (NDP), number of participants without disabilities; N (PWD), number of participants have disabilities; *w*, passage width.

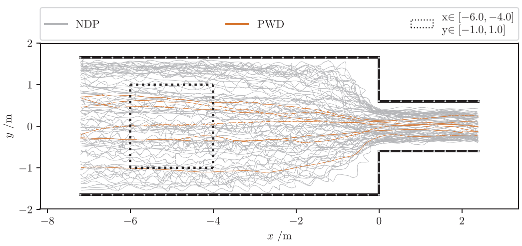

(A) Bot_whe_08: ≈ 10 % wheelchair users.

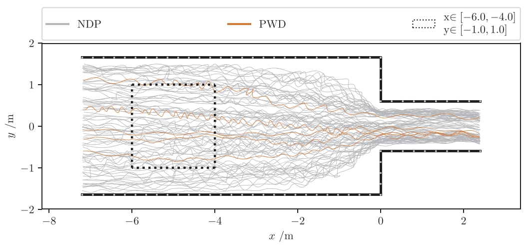

(B) Bot_wal_08: ≈ 10 % with walking disabilities.

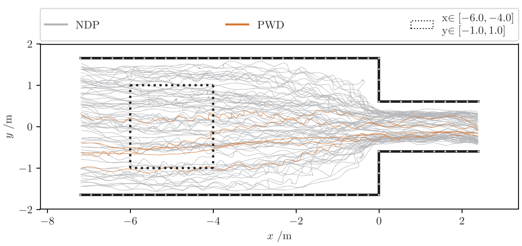

(C) Bot_mix_08: ≈ 10 % with mixed (single) disabilities.

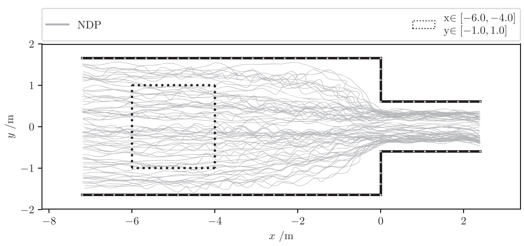

(D) Bot_ref_08: no participants with disabilities.

FIGURE 3 Trajectories for (A) Bot_whe_08 with approximate 10% of participants using a wheelchair, (B) Bot_wal_08 with approximate 10% of participants with walking disabilities, (C) Bot_mix_08 with approximate 10% of participants with mixed (single) disabilities, and (D) for Bot_ref_08 without participants with disabilities. The passage width is 1.2 m and the measurement area is plotted by the black rectangle. Coordinates of the measurement area are given in the angular brackets [Colour figure can be viewed at wileyonlinelibrary.com]

above the entrance of the bottleneck perspective. For details of the error calculation, we refer to Appendix 2 and Boltes et al.[51]

Trajectory data is available at the pedestrian dynamics data archive and can be accessed with http://ped.fz-juelich.de/da/2017sime.

2.3 | Measurement

Based on the individual position and the time step, the participants can be represented as a set of points in the metric space, which can be transferred into a Voronoi diagram.[53,54] The Voronoi tessellation assigns an individual required space to each person (called Voronoi cell $A_i(t)$) which includes all coordinates of the Euclidean plane that are closer to the participant i than to the neighbours.[54-56] In addition, the Voronoi cell is controlled by walls, obstacles, and generally also by a cutoff (here set to 2.0m) radius that represents the participant's maximum sphere of influence. In order to consider interactions with the boundaries of the built-environments, virtual geometry points are additionally defined, which are interpreted as "virtual neighbours" and that are also included when calculating the Voronoi cells. These geometry points are defined on the walls with an increment of 0.25 m to consider boundary effects when a person is walking close to the wall. The lower the distance between the virtual neighbours on the wall, the smaller the Voronoi cell of the passing person. With increments of 0.25 m, a natural distance between a person's cell and the wall is

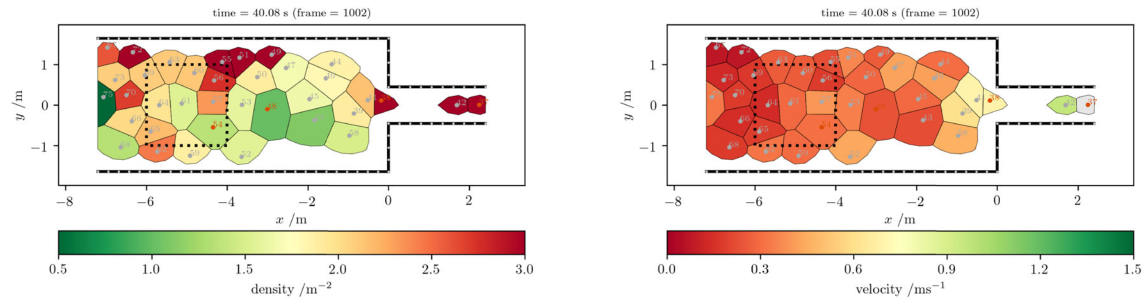

(A) ρ_v for Bot_whe (B) v_v for Bot_whe

FIGURE 4 Voronoi density ρ_v (left) and movement speed v_v (right) for Bot_whe. The trajectory points and individual identification numbers of participants are annotated in grey (NDP) and orange (PWD) [Colour figure can be viewed at wileyonlinelibrary.com]

maintained while the cell around the wall point is not weighted too strongly (compared with interactions with real neighbours).

Thus, the density and movement speed distribution of the area is

$$\rho_i(x,y,t) = \begin{cases} \frac{1}{A_i}(t) & : \quad \forall (x,y) \in A_i(t) \\ 0 & : \quad \text{other} \end{cases} \tag{1}$$

and

$$v_i(x,y,t) = \begin{cases} v_v(t) & : \quad \forall (x,y) \in A_i(t) \\ 0 & : \quad \text{other.} \end{cases} \tag{2}$$

The density within the Voronoi cell $A_i(t)$ of a participant i is calculated as the reciprocal of the area content of the cell. This makes it possible to weight the influence of individual parts of neighbouring participants on the measuring area. With the densities and movement speeds related to individual position points, the Voronoi density ρ_v (Equation 3) and Voronoi velocity v_v (Equation 4) are obtained at time t on the measuring area $\Delta x \cdot \Delta y$ as follows:

$$\rho_v(x,y,t,\Delta x,\Delta y) = \frac{\iint \rho_i(x,y,t)dxdy}{\Delta x \cdot \Delta y}, \tag{3}$$

$$v_v(x,y,t,\Delta x,\Delta y) = \frac{\iint v_i(x,y,t)dxdy}{\Delta x \cdot \Delta y}. \tag{4}$$

A detailed error estimation for these methods is difficult to make since there are many influencing factors. While the small error in trajectory extraction is negligible, an increased error is made by the approximation of the individual required space by Voronoi cells as individual physiques are not considered and the kept distance to the wall is challenging to reproduce. In addition, the resulting density and movement speed are sensitive to the position of the measurement area and a valid time interval for the analysis. Nevertheless, the described methods are a proven approach for analysis and have been used in many prior studies, for instance in Germany,[4,53,54,57-71] Australia[72-77] Japan,[78-80] Palestine[81] and China.[31-33,82,83]

An example for the distribution of Voronoi density and movement speed over space in a bottleneck (at time step 40.08 s which is similar to frame 1002) for a study with and without wheelchair users is presented in Figure 4.

3 | ANALYSIS AND RESULTS

3.1 | Unimpeded movement speed

Before performing an experimental trial with a new subpopulation, each participant (NDP and PWD) passed the study setting alone. Therefore, the distance between the individuals was controlled by an instructor with respect to interpersonal distance of approximately 5 s, which is similar to approximately 6m interpersonal space (expecting a free movement speed of 1.2ms^{-1}). The unimpeded movement speed v_0 of each participant was measured. Distributions of the unimpeded movement speeds depending on the population are presented in Figure 5.

Overall, the observed unimpeded movement speeds of NDP are 1.47±0.17 ms^{-1} and comparable with literature findings (see Gwynne and Boyce[6] or Geoerg et al[13]). On the other hand, unimpeded movement speeds of the PWD depends strongly on individual characteristics such as the kind of movement ability or flexibility in manoeuvring with assistive devices which leads to high standard deviations (see for instance the different shapes of the distributions in Figure 5A-C). The unimpeded movement speed for wheelchair users was 0.96±0.35 ms^{-1}, for participants with walking disabilities 1.28±0.12 ms^{-1}, and for participants with mixed disabilities 1.33±0.29 ms^{-1}.

3.2 | Stationarity and stability

In general, parameters like a pedestrian flow rate are not constant in time because of individual characteristics and social interrelations. So, in practice, long measurement intervals reduce the fluctuations and short measurement intervals reduce the statistical meaning of the observed phenomena.[84-86] While in field studies of car traffic periods of 3 to 5 minutes are not uncommon for the determination of moving averages,[84] controlled studies of pedestrian dynamics usually have significantly shorter running times due to limited personnel and financial factors which is unlike in field studies of vehicle traffic. Thus, a significant part of the time period depends on (random distributed) start and end conditions (eg, low densities and movements lower than the free flow state at the beginning and the end of a trial).

As discussed in more detail in Geoerg et al[42] a central aim of this study was the comparison of influences by different types of population heterogeneities, which are in nature characterised by

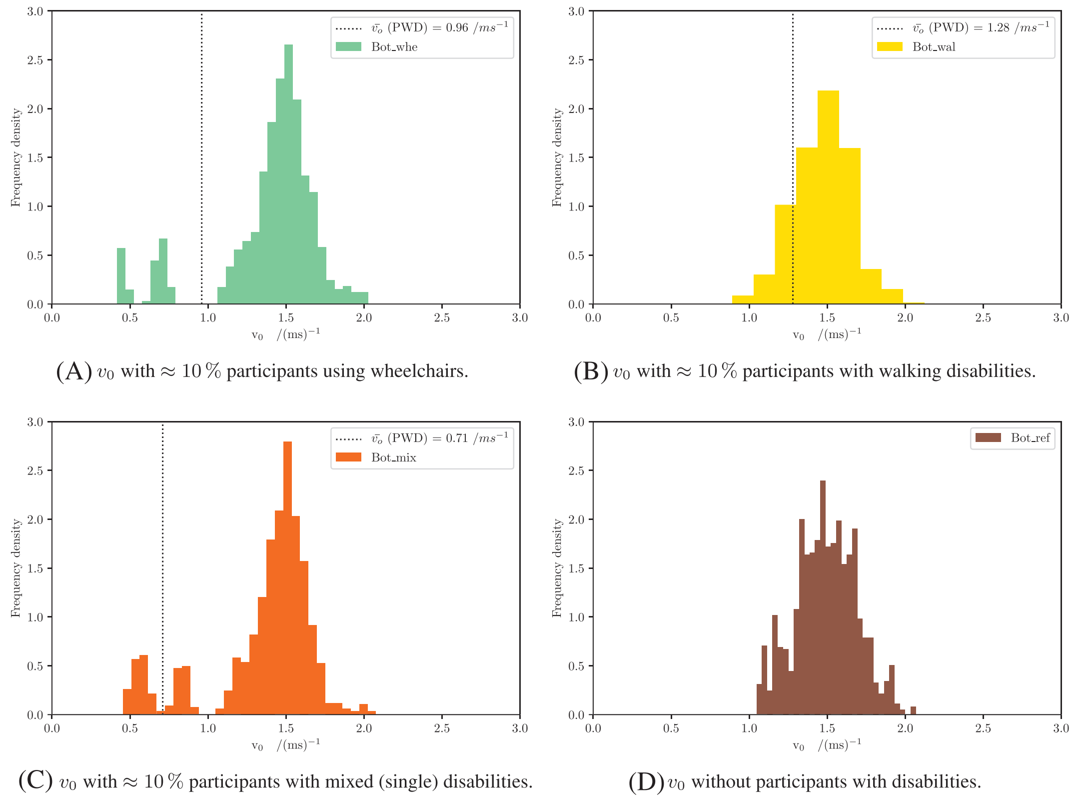

(A) v_0 with ≈ 10 % participants using wheelchairs.

(B) v_0 with ≈ 10 % participants with walking disabilities.

(C) v_0 with ≈ 10 % participants with mixed (single) disabilities.

(D) v_0 without participants with disabilities.

FIGURE 5 Frequency densities of unimpeded movement speeds in ms^{-1} for different subpopulations. The unimpeded movement speed of the subpopulations considering participants with disabilities is plotted by the dotted vertical line and is for wheelchair users 0.96±0.35 ms^{-1}, for walking disabled participants 1.28±0.12 ms^{-1}, for participants with mixed disabilities 1.33±0.29 ms^{-1}, and for participants without any disability 1.47±0.17 ms^{-1}. For a detailed analysis of the data, we kindly refer to Geoerg et al[42] [Colour figure can be viewed at wileyonlinelibrary.com]

fluctuations in time-dependent parameters. For this reason, intervals of relative stable conditions were defined manually in this analysis. This was realised by a qualitative time series analysis for movement speed, density, and flow rate (in accordance to previous studies[56,63,87-90]) and results in different measuring surfaces in time (see differences in the gray coloured area in Figure 6). In constant space-dimension, we took the measurement in a rectangular area in a distance of 4.0 m to the bottleneck entrance (Figures 2 and 3).

Overall densities in a range between 2.0 and 3.0 m^{-2} were observed in all configurations (varied width and subpopulations) with low average movement speeds and moderate flows. The ladder can be justified by a manageable number of participants and, as a result of a two-day-cooperation, a polite and considerate behaviour and the low motivation of the participants. Focussing the time development of the studies with the reference population, the measured performance criteria does not show remarkable fluctuations: the flow inside the measurement area increases after start, goes to a small steady state condition plateau of approximately 10 s, and decreases afterwards. The appearance of the average values is harmonious without noticeable fluctuations (Figure 6D). If subpopulations of PWD were considered, density increases within 25 s from initial density up to a local maximum and remains steady (but fluctuating) for approximately 40 s (Figure 6A, considering wheelchair users), approximately 20 s (Figure 6B, considering walking disabled participants), or approximately 10 s (Figure 6C, considering mixed subpopulation). But the appearance of the time-dependent development changes, if PWD were considered: remarkable fluctuations, especially in the average density and flow, are observed (see for instance time stamp 30 s or time stamp 55 s in Figure 6A). In consequence, the process of obtaining the empirical relations must consider the data of PWD (fluctuating data) and the need for stable conditions (steady states).

In order to place the measurement area in a region of the study setup where stable conditions can be achieved, the spatio-temporal dependency of the measures were analysed. To implement this, a mesh grid of 600 × 600 cells was distributed over the geometrical setup and the time-dependent values were linear interpolated for each frame during the steady state interval. Figure 7 shows the flow rate profiles for the four different populations in a bottleneck with a passage width of 0.9 m. The observed maximum individual flow is approximately 2.5 s^{-1} for all populations. It is worth noticing that the maximum flow was observed at the entrance to the bottleneck and that the flow in front of the bottleneck is lower than inside the bottleneck (which is in accordance to the findings by Zhang and Seyfried[89]). As expected, the flow rate is not homogeneously distributed over the entire space for all configurations: throughout analysing the study with a reference population (Figure 7), walking disabled (Figure 7), and mixed-population (Figure 7), the flow decreases mainly near to the bottleneck entrance due to increasing density in front of the bottleneck. But, if a subpopulation using wheelchairs is considered, the situation is quite different (Figure 7): a decreased flow rate is observable over the entire geometry which is independent from the observed passage width. Therefore, higher densities occur along the entry hall which confirms that the mode of movement is different.

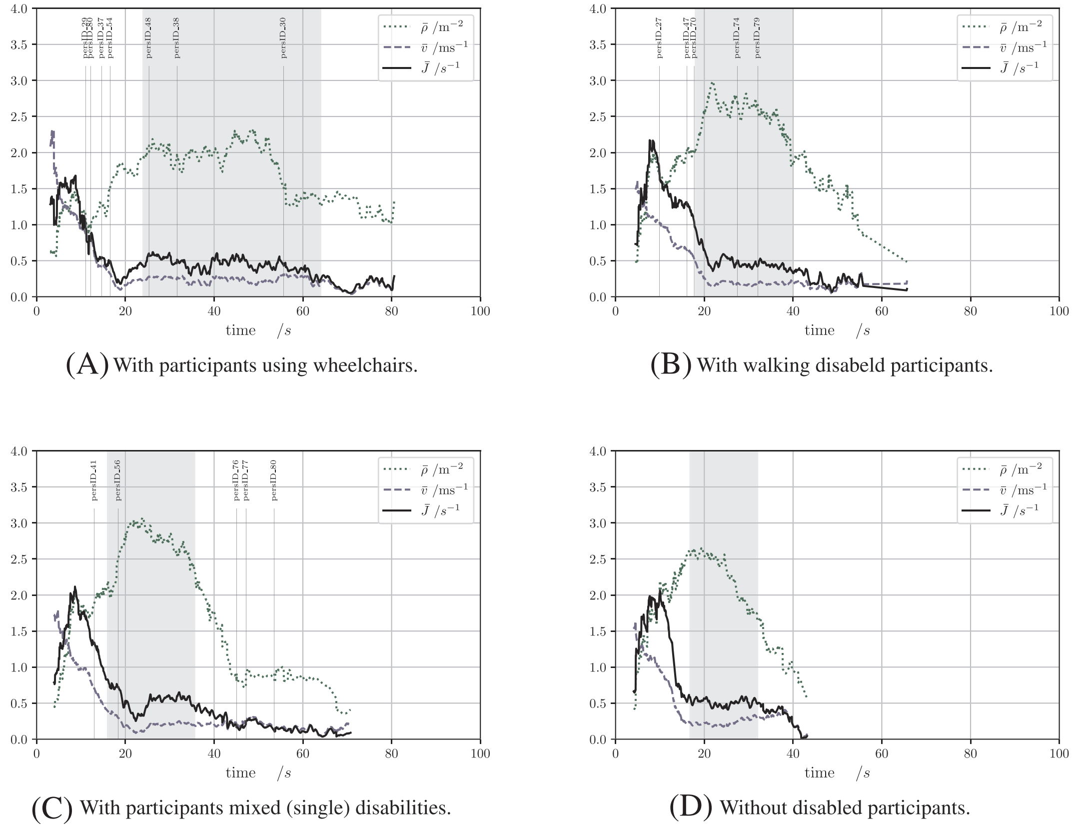

(A) With participants using wheelchairs.

(B) With walking disabeld participants.

(C) With participants mixed (single) disabilities.

(D) Without disabled participants.

FIGURE 6 Time series of moving average measures $\bar{\rho}(t)$, $\bar{v}(t)$, and $\bar{J}(t)$ in a time interval of 2 seconds (which is corresponding to 50 frames) for bottleneck configurations with a passage width of 0.9 m and different subpopulations (top left: wheelchair users, top right: walking disabled, bottom left: mixed disabilities and bottom right: reference population without disabilities). The persID and the time of entrance of participants with disabilities into the measurement area is emphasised by the vertical lines. The period of stationary conditions is presented by the grey coloured area. For a more detailed description of the characteristics of the persID, see Georg et al.[52] [Colour figure can be viewed at wileyonlinelibrary.com]

Concluding, the observed flow during the consideration of wheelchair users may not be the capacity of the built-environment.

4 | CAPACITY ANALYSIS

We focus on the analysis of the fundamental relationship of $v(\rho)$ and $J(\rho)$ for unidirectional movement through the bottleneck geometries with different subpopulations. The derived fundamental diagrams for $\bar{v}(\bar{\rho})$ and $\bar{J}(\bar{\rho})$ are determined by the stationary states resulting from the time series analysis (Figure 6). A time interval of 2 seconds (which is corresponding to 50 frames) was used to calculate the simple moving averages (SMA) of the entire data points. For clarification, data is presented in dependence of the experimental trials and the different widths in App. A.

As a result of the limited number of participants, the observed density interval is in between 0.5 and 5.0 m^{-2}. The lower threshold of density located at 0.5 m^{-2} is due to the fact that the size of Voronoi cells was limited to a maximum length (cut-off-radius) of 2.0 m to avoid infinitely long Voronoi cells at lower densities. Given only one participant in a measurement area of 4.0 m^2 does lead to $\rho = \frac{MA}{A_i} = 0.5$, which defines the threshold value.

In-depth analysis of individual data points regarding the participants showed that participants with walking and mixed disabilities are likely to appear in all density regions (Bot_wal and Bot_mix). This observation does not apply to the results of the Bot_whe study, where wheelchair users are considered. Participants in wheelchairs tend to appear in density regions less than 2.0 m^{-2}. Otherwise, participants with mixed disabilities are distributed over a density up to 4.0 m^{-2}.

The resulting empirical relations $\bar{v}(\bar{\rho})$ and $\bar{J}(\bar{\rho})$ are presented in Figure 8 to 11. The overall data for each experimental trial is presented by the scatter, supplemented by a visualisation of the two-dimensional (gaussian) density plot of the data (red lines). The one-dimensional distribution on speed and density or flow rate and density are presented, respectively, at the marginals. Results of a polynomial regression analysis is presented by the blue line plot. It is worth noticing that the observed average movement speed is low for all configurations (approximately 0.25 ms^{-1}).

A slight linear dependency of $\bar{v}(\bar{\rho})$ was observed for the reference population (Figure 11) for movement in groups with disabled subpopulations a nonlinear dependency was observed (Figures 8-10). While considering participants with mixed disabilities and without disabilities, a dependency between movement speed and density is recognisable over the entire density, the averaged movement speed of populations with wheelchair users and walking disabled participants is independent from densities greater than 1.5 m^{-2}. This is in contrast to the expected behaviour and data from previous studies with homogeneous populations (eg, previous studies[9,57,91]) and the classic understanding of the fundamental diagram where dependency between movement speed and density is expected.

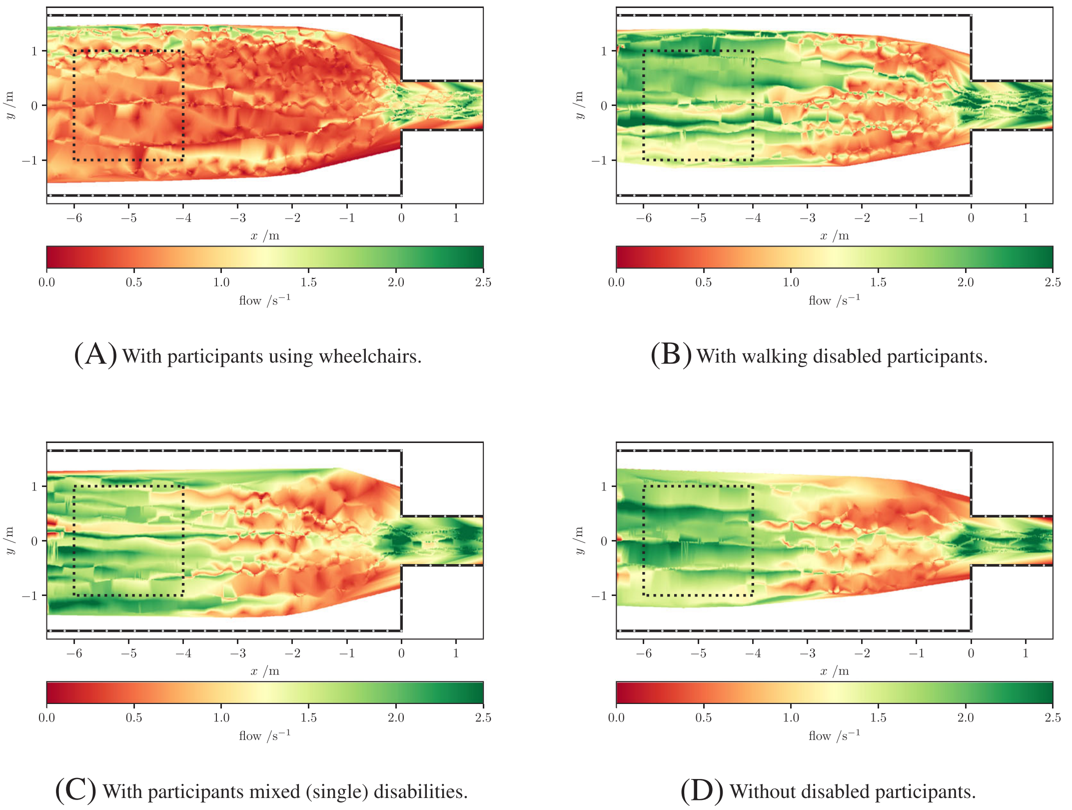

FIGURE 7 Profile plot (mesh grid size: 600 × 600, linear interpolation method) of the flow rate in a bottleneck configuration (passage width of 0.9 m) for different populations during the stationary states. Approximately 10% of participants using a wheelchair (top left), participants with walking impairments (top right), participants with mixed disabilities (bottom left), and a reference population without participants with disabilities (bottom right) [Colour figure can be viewed at wileyonlinelibrary.com]

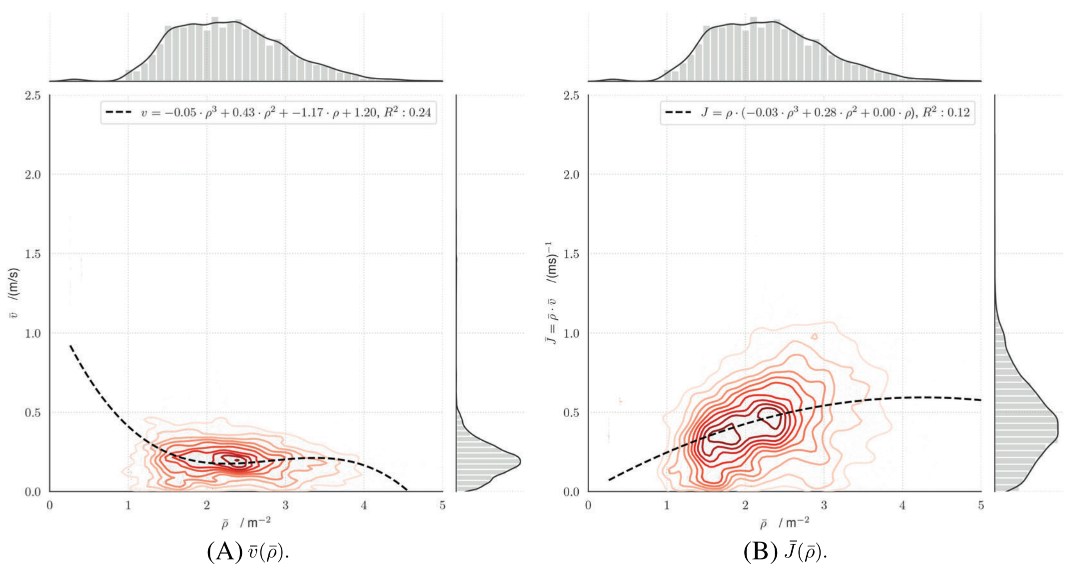

FIGURE 8 Empirical relations $\bar{v}(\bar{\rho})$ and $\bar{J}(\bar{\rho})$ for Bot_whe. Overall data of each experimental trial plotted by the scatter. The red lines are the visualisation of the two dimensional (gaussian) density plot of the data. The one-dimensional distribution on speed and density or flow rate and density is presented, respectively, at the marginals. Last, results of a polynomial regression analysis is presented by the blue line plot [Colour figure can be viewed at wileyonlinelibrary.com]

The comparison of individual fundamental diagrams $\bar{J}(\bar{\rho})$ is presented in Figure 8A to Figure 11A. As indicated by results of the $\bar{v}(\bar{\rho})$-analysis and with respect to the overall slow movement speeds, low flow rates J were observed for all configurations. In general, a dependency of the flow on density was observed for all configurations. Considering the population with mixed (single) disabled participants and the reference population only, the capacity was reached where the critical density ρ_c was approximately 2.2 m^{-2}. Surprisingly, the shape of the fitting

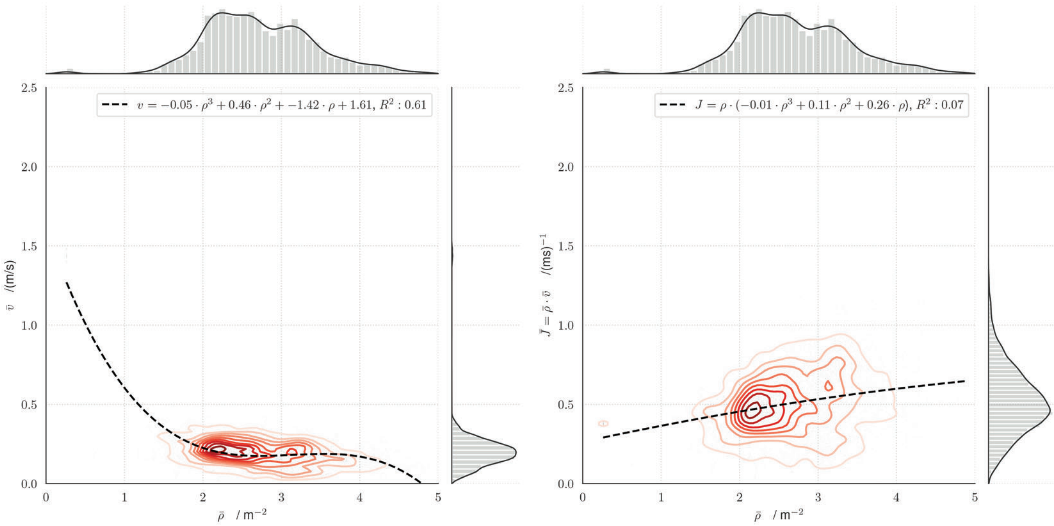

(A) $\bar{v}(\bar{\rho})$. (B) $\bar{J}(\bar{\rho})$.

FIGURE 9 Empirical relations $\bar{v}(\bar{\rho})$ and $\bar{J}(\bar{\rho})$ for Bot_wal [Colour figure can be viewed at wileyonlinelibrary.com]

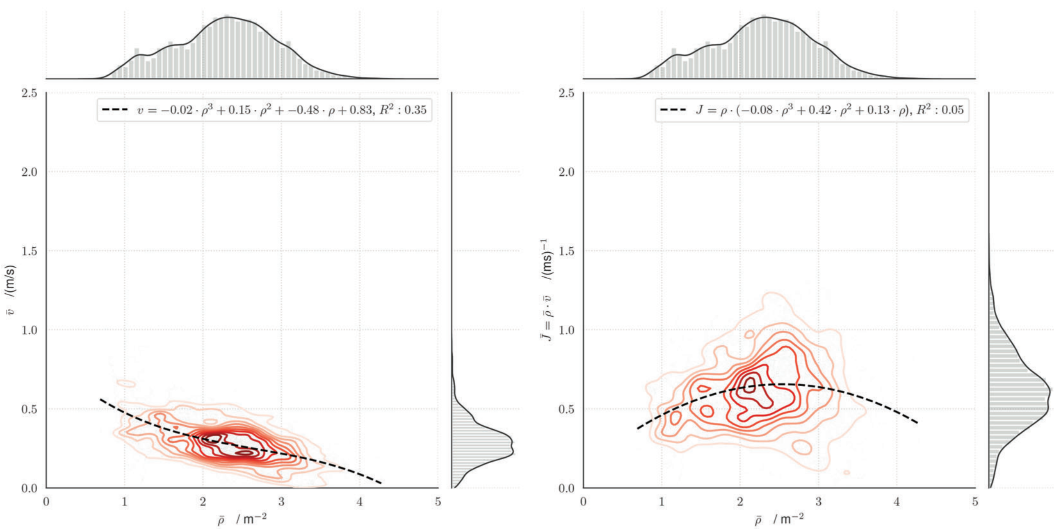

(A) $\bar{v}(\bar{\rho})$. (B) $\bar{J}(\bar{\rho})$.

FIGURE 10 Empirical relations $\bar{v}(\bar{\rho})$ and $\bar{J}(\bar{\rho})$ for Bot_mix [Colour figure can be viewed at wileyonlinelibrary.com]

curves for populations with wheelchair users and walking disabled participants totally differ from the expected quadratic shape. Even more, the capacity was not reached for these populations even if the size of the population was comparable (compare the number of participants of each study in Table 1). Here, the observed flow rate increase rather linearly. The flow rate here is much less dependent from the width than for population with mixed single disabilities or the reference population (see the spatial distribution, especially in y-direction of similar coloured points in Figures 1 and 2).

A small scatter in the distribution of movement speed and flow rates for the studies considering participants in wheelchairs or participants with walking disabilities are striking out (see histogram on the y-axis [in left column of Figures 8A-11A]: these subpopulations are characterised by participants whose disability is visible to others [see narrative description of participants of these experimental trials in Geoerg et al[52]]). Such a combination of participant's familiarity and visibility of "need for assistance" to others leads to a communicative, considerate behaviour between participants in wheelchairs and nondisabled participants. In result, the movement speed of all participants were anticipated to the movement speed of the slower wheelchair users.[42] In these studies, the subgroup of PWD and NDP interact and solve priority of movement by communication. An estimation of the influence of heterogeneity on the empiric relations is not easily feasible. The well-controlled system of variables in unidirectional movement is here altered by the degrees of freedom because of altered individual space requirement, variable (social) distances, and interactions. This results in a complex dynamic system where the influence of a (controlled) variable (eg, ρ) on a target variable (here, v or J) is no longer given. This behaviour by NDP was only observed–qualitatively by video analysis and reflecting in results of fundamental relationships $\bar{v}(\bar{\rho})$ and $\bar{J}(\bar{\rho})$—if participants with visible disabilities indicated by

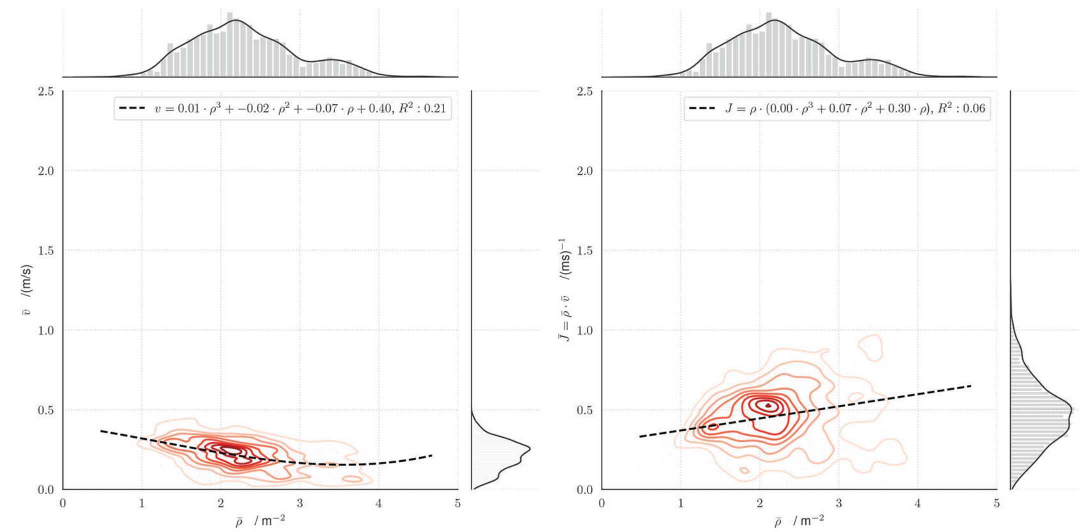

(A) $\bar{v}(\bar{\rho})$. (B) $\bar{J}(\bar{\rho})$.

FIGURE 11 Empirical relations $\bar{v}(\bar{\rho})$ and $\bar{J}(\bar{\rho})$ for Bot_ref [Colour figure can be viewed at wileyonlinelibrary.com]

assistive devices or recognisable characteristic such as spasticity or uncontrolled behaviour are part of the subpoulation.

5 | CONCLUSION AND OUTLOOK

A series of well-controlled studies on movement through a bottleneck was performed. The influence of variably composed subpopulations and a varied passage width on the fundamental relationships $\bar{v}(\bar{\rho})$ and $\bar{J}(\bar{\rho})$ was analysed.

The unimpeded movement speed of all participants was measured and analysed with respect to the individual abilities. Expected unimpeded movement speeds of 1.47 ± 0.17 ms^{-1} were observed with the nondisabled reference population which is consistent with the literature.[13] Focusing on the unimpeded movement speed of the subpopulations with different disabilities, a slower, in case of the subpopulation consists of wheelchair users (Bot_whe: 0.96 ± 0.35 ms^{-1}) or comparable (Bot_wal: 1.28 ± 0.12 ms^{-1} and Bot_mix: 1.33 ± 0.29 ms^{-1}) average unimpeded movement speed was measured.

Further on, the fundamental relationships $\bar{v}(\bar{\rho})$ and $\bar{J}(\bar{\rho})$ were studied. Because of the experimental boundary conditions, a maximum flow point (capacity) was not reached. Thus, the free flow branch of the fundamental diagram was studied. It was found that the shape of the speed-density relation is different to previously research in case of participation of wheelchair users. This uncommon characteristic results from a polite and considerate (social) behaviour of nondisabled participants, if participants whose disability is visible to others participate (eg, wheelchair users). Additional space in case of larger passage widths has no effects of performance criteria of wheelchair users because the additional space is to leak for overtaking or passing the line simultaneously. The relationship $\bar{J}(\bar{\rho})$ results in a slightly linear correlation which is independent of the considered subpopulation and even true in case of consideration of wheelchair users. This effect results from an increased individual density at a given (anticipated and constant) movement speed.

Different shapes in the distributions, differing maxima, and an additional influencing parameter underlines the outstanding importance of sensitivity analyses in the interpretation of results by engineering egress calculation methods.

It is worth mentioning that the number of data for the wheelchair users is limited and that usage of larger steps of additional widths (eg, a multiple of a wheelchair width) may have an impact on the flow. Differences in mobility characteristics may lead to issues when considering these individual properties in calculation methods. Differences in mobility characteristics may lead to issues when considering these individual properties in calculation methods. But, the results presented may be a first step to be used to improve engineering egress calculations under consideration of different configurations of populations in design and planning process of facilities. Further research, especially on the comparison between different processes in movement and different ratios of populations, is required.

Real situations are characterised by an increased complexity and interaction of different influencing variables, which are deliberately reduced in the controlled boundary conditions. Needless to say, the nature of the well-controlled setting may differ from crowd behaviour during real events. A scaling of effects observed and quantified in laboratory studies to real events should always be carried out with caution and critical evaluation of the boundary conditions. Finally, studies with controlled boundary conditions are only models of more complex scenarios and should be considered as such.

DATA AVAILABILITY STATEMENT

Trajectory data is published at the pedestrian dynamics data archive and can be accessed with http://doi.org/10.34735/PED.2017.1.

FUNDING STATEMENT

This work has been performed within the research programme "Sicherheit für Menschen mit körperlichen, geistigen oder altersbedingten Beeinträchtigungen (SiME)" funded by the German Federal Ministry of Education and Research - BMBF (grant numbers 13N13946 and

13N13950). P.G. thanks the SFPE Foundation for financial support with the Dr Guylène Proulx, OC Scholarship.

ACKNOWLEDGEMENTS

We thank the team and employees of the Lebenshilfe Bergisches Land and the anonymous participants for the committed and patient support during planning and conduction of the movement studies.

ORCID

Paul Georeg https://orcid.org/0000-0001-7196-1245
Jette Schumann https://orcid.org/0000-0003-3668-999X
Maik Boltes https://orcid.org/0000-0001-7240-896X
Anja Hofmann https://orcid.org/0000-0002-1168-6701

REFERENCES

1. Thompson P, Nilsson D, Boyce K, McGrath D. Evacuation models are running out of time. *Fire Safety J*. 2015;78:251-261. https://doi.org/10.1016/j.firesaf.2015.09.004
2. Boyce K. Safe evacuation for all—fact or fantasy? Past experiences, current understanding and future challenges: past experiences, current understanding and future challenges. *Fire Safety J*. 2017;91:28-40. https://doi.org/10.1016/j.firesaf.2017.05.004
3. Kuligowski E. Burning down the silos: integrating new perspectives from the social sciences into human behavior in fire research. *Fire Mater*. 2017;41(5):389-411. https://doi.org/10.1002/fam.2392
4. Sieben A, Schumann J, Seyfried A. Collective phenomena in crowds—where pedestrian dynamics need social psychology. *PloS one*.2017;12(6):e0177328. https://doi.org/10.1371/journal.pone.0177328
5. Hofinger G, Zinke R, Schröder B, Andresen E, Künzer L. Human factors in pedestrian simulation: field studies in underground stations. In: Proceedings of the 8th International Conference on Pedestrian and Evacuation Dynamics Song W, Ma J, Fu L, eds.; 2016; Hefei, China.
6. Gwynne S, Boyce K. E.. Engineering Data. In: Hurley MJ, ed. *SFPE Handbook of Fire Protection Engineering*. New York: Springer; 2016:2429-2551.
7. Boyce K. Panel: Fundamentals of egress calculations for life safety for egress assessments. *Fire and Materials*. 2015;39(4):466-474. https://doi.org/10.1002/fam.2301
8. Shi X, Ye Z, Shiwakoti N, Grembek O. A state-of-the-art review on empirical data collection for external governed pedestrians complex movement. *J Adv Trans*. 2018;2018(2):1-42. https://doi.org/10.1155/2018/1063043
9. Boltes M, Zhang J, Tordeux A, Schadschneider A, Seyfried A. Empirical results of pedestrian and evacuation dynamics. In: Meyers RA, ed. *Encyclopedia of complexity and systems science*, Springer Reference, vol. 16; 2018:1-29. https://doi.org/10.1007/978-3-642-27737-5_706-1
10. Haghani M, Sarvi M. Crowd behaviour and motion: empirical methods. *Trans Res Part B Methodological*. 2018;107:253-294. https://doi.org/10.1016/j.trb.2017.06.017
11. Zhou M, Dong H, Ning B, Wang F. Recent development in pedestrian and evacuation dynamics: bibliographic analyses, collaboration patterns, and future directions. *IEEE Trans Comput Soc Syst*. 2018;5(4):1034-1048. https://doi.org/10.1109/TCSS.2018.2878102
12. Fahy R. Panel: life safety options for people with disabilities—how far have we come. *Fire and Materials*. 2015;39(4):475-485. https://doi.org/10.1002/fam.2300
13. Geoerg P, Berchtold F, Gwynne S, Boyce K, Holl S, Hofmann A. Engineering egress data considering pedestrians with reduced mobility. *Fire Mater ls*. 2019;43(7):759-781. https://doi.org/10.1002/fam.2736
14. Hashemi M, Tomasiello S. Emergency evacuation of people with disabilities: a survey of drills, simulations, and accessibility. *Cogent Eng*. 2018;5(1):1-20. https://doi.org/10.1080/23311916.2018.1506304
15. Sørensen J., Dederichs A. Evacuation characteristics of visually impaired people—a qualitative and quantitative study. *Fire Mater*. 2013;39(4):385-395. https://doi.org/10.1002/fam.2200
16. Sørensen J., Dederichs A. Evacuation characteristics of visually impaired people—a qualitative and quantitative study. *Fire and Mater*. 2015;39(4):385-395. https://doi.org/10.1002/fam.2200
17. Samoshin D, Istratov R. The characteristics of blind and visually impaired people evacuation in case of fire. *Fire Safety Sci*. 2014;11:1160-1169. https://doi.org/10.3801/IAFSS.FSS.11-1160
18. Cao S, Fu L, Song W. Exit selection and pedestrian movement in a room with two exits under fire emergency. *Appl Math Comput*. 2018;332:136-147. https://doi.org/10.1016/j.amc.2018.03.048
19. Cao S, Wang P, Yao M, Song W. Dynamic analysis of pedestrian movement in single-file experiment under limited visibility. *Commun Nonlinear Sci Numer Sim*. 2019;69:329-342. https://doi.org/10.1016/j.cnsns.2018.10.007
20. Sharifi M, Stuart D, Christensen K, Chen A. Traffic flow characteristics of heterogeneous pedestrian stream involving individuals with disabilities. *Trans Res Rec J Trans Res Board*. 2015;2537:111-125. https://doi.org/10.3141/2537-13
21. Shields T, Boyce K, Silcock G, Dunne B. The impact of a wheelchair bound evacuee on the speed and flow of evacuees in a stairway during an uncontrolled unannaunced evacuation. *J Appl Fire Sci*. 1997;7(1):29-39. https://doi.org/10.2190/2DG0-RHKQ-PD1V-3HNW
22. Tsuchiya S, Hasemi Y, Furukawa Y. Evacuation characteristics of group with wheelchair users. *Proc Asia-Oceania Sym Fire Sci Technol*. 2007;7:117-117.
23. Sharifi M, Stuart D, Christensen K, Chen A, Kim YS, Chen Y. Analysis of walking speeds involving individuals with disabilities in different indoor walking environments. *J Urban Plan Dev*. 2016;142(1):04015010. https://doi.org/10.1061/(ASCE)UP.1943-5444.0000288
24. Daamen W, Hoogendoorn S. Capacity of doors during evacuation conditions. *Procedia Eng*. 2010;3:53-66. https://doi.org/10.1016/j.proeng.2010.07.007
25. Larusdottir A, Dederichs A. A step towards including children's evacuation parameters and behavior in fire safe building design. *Fire Safety Sci*. 2011;10:187-195. https://doi.org/10.3801/IAFSS.FSS.10-187
26. Daamen W, Hoogendoorn S. Emergency door capacity: influence of door width, population composition and stress level. *Fire Technol*. 2012;48(1):55-71. https://doi.org/10.1007/s10694-010-0202-9
27. Daamen W, Hoogendoorn S. Calibration of pedestrian simulation model for emergency doors by pedestrian type. *Trans Res Record: J Trans Res Board*. 2012;2316(1):69-75. https://doi.org/10.3141/2316-08
28. Kholshevnikov V, Samoshin D, Parfyonenko A, Belosokhov I. Study of children evacuation from pre-school education institutions. *Fire and Mater*. 2012;36(5-6):349-366. https://doi.org/10.1002/fam.2152
29. Kholshevnikov V, Samoshin D, Istratov R. The problems of elderly people safe evacuation from senior citizen health care buildings in case of fire. In: Shields TJ, ed. *Human behaviour in fire*. London: Interscience Communications; 2012:587-593.
30. Larusdottir A, Dederichs A. Evacuation of children: movement on stairs and on horizontal plane. *Fire Technology*. 2012;48(1):43-53. https://doi.org/10.1007/s10694-010-0177-6
31. Cao S, Zhang J, Salden D, Ma J, Shi C, Zhang R. Pedestrian dynamics in single-file movement of crowd with different age compositions. *Physical Rev E*. 2016;94(1). https://doi.org/10.1103/PhysRevE.94.012312

32. Cao S, Zhang J, Song W, Shi C, Zhang R. The stepping behavior analysis of pedestrians from different age groups via a single-file experiment. *J Stat Mech Theory Exp*. 2018;2018(3):033402. https://doi.org/10.1088/1742-5468/aab04f
33. Ren X, Zhang J, Song W, Cao S. The fundamental diagrams of elderly pedestrian flow in straight corridors under different densities. *J Stat Mech Theory Exp*. 2019;2019(2):023403. https://doi.org/10.1088/1742-5468/aafa7b
34. The United Nations Office for Disaster Risk Reduktion, ed.. Living with Disability and Disaster: UNISDR 2013 Survey on Living with Disabilities and Disasters: Key Findings.
35. Klynman Y, Kouppari N, Mukhier M, eds. *World Disasters Report: Focus on Discrimination*, World Disasters Report, vol. 2007. Geneva, CH: International Federation of Red Cross & Red Crescent Societies Switzerland; 2007.
36. Christensen K, Collins S, Holt J, Phillips C. The relationship between the design of the built environment and the ability to egress of individuals with disabilities. *J Disabil Policy Stu*. 2007;2(3):24-35.
37. Cutter S, Finch C. Temporal and spatial changes in social vulnerability to natural hazards. *Proc Nati Acad Sci U S A*. 2008;105(7):2301-2306. https://doi.org/10.1073/pnas.0710375105
38. Klippel A, Rabe F, Krause U, Hofmann A. Quantitative risk analysis and numerical investigation to determine critical fire scenarios in the environment of people with disabilities. In: Grayson S, ed. *INTERFLAM 2019*. London: Interscience Communications; 2019:795-806.
39. Klippel A, Rabe F, Krause U, Hofmann A. Quantitative risk analysis and numerical investigation to determine critical fire scenarios in the environment of people with disabilities: (under review). *Fire and Mater*. 2019.
40. Kelman I, Stough LM, eds. *Disability and Disaster: Explorations and Exchanges*. New York, NY: Palgrave Macmillan; 2015.
41. Internation Federation of red cross and red crescent societies, ed.. *World Disaster Report 2009: Focus on early warning, early action*. Geneva and Switzerland; 2009.
42. Geoerg P, Schumann J, Holl S, Hofmann A. The influence of wheelchair users on movement in a bottleneck and a corridor. *Journal of Advanced Transportation*. 2019;2019(3):1-17. https://doi.org/10.1155/2019/9717208
43. Geoerg P, Block R, Heister W, Holl S, Pulm A, Hofmann A. A score regarding the need for assistance: considering pedestrians with disabilities in evacuation planning. In: Proceedings of the 5th Magdeburg Fire and Explosion Prevention Day Krause U, Rost M, eds.; 2017; Magdeburg and Germany.
44. Geoerg P, Block R, Heister W, Holl S, Pulm A, Hofmann A. A score regarding the need for assistance—evacuation considering people with disabilities: (under review). *Fire Safety Journal*. 2019.
45. Statistisches Bundesamt. *Bevölkerung und Erwerbstätigkeit: Bevölkerungsfortschreibung auf Grundlage des Zenzus 2011: Fachserie 1 Reihe 1.3*. Wiesbaden; Statistisches Bundesamt; 2015.
46. Statistisches Bundesamt. *Sozialleistungen: Schwerbehinderte Menschen: Fachserie 13; Reihe 5.1*. Wiesbaden; Statistisches Bundesamt; 2019.
47. *World report on disability*. Geneva: WHO; World Health Organization; 2011.
48. Eurostat Statistics Explained, EUROSTAT, eds. *Disability statistics - need for assistance*; 2015. https://ec.europa.eu/eurostat/statistics-explained/index.php?title=Disability_statistics_-_need_for_assistancePeople_with_disabilities_requiring_assistance
49. Brault M. Americans With Disabilities: 2010: Report Number P70-131. 2012. https://www.census.gov/library/publications/2012/demo/p70-131.html%
50. Boltes M, Seyfried A. Collecting pedestrian trajectories. *Neurocomputing*. 2013;100:127-133. https://doi.org/10.1016/j.neucom.2012.01.036
51. Boltes M, Holl S, Tordeux A, Seyfried A, Schadschneider A, Lang U. Influences of extraction techniques on the quality of measured quantities of pedestrian characteristics. In: Proceedings of the 8th International Conference on Pedestrian and Evacuation Dynamics Song W, Ma J, Fu L, eds.; 2016; Hefei,C:540-547.
52. Geoerg P, Schumann J, Holl S, Boltes M. Influence of Individual Characteristics on Movement in a Bottleneck and a Corridor: Extended documentation on large-scale movement studies. http://ped.fz-juelich.de/data/experiments/2017.06.10_Wermelskirche%n_SiME/docu/data_documentation/docu.pdf
53. Zhang J, Klingsch W, Schadschneider A, Seyfried A. Transitions in pedestrian fundamental diagrams of straight corridors and T-junctions. *J Stat Mech Theory Exp*. 2011;2011(06):P06004. https://doi.org/10.1088/1742-5468/2011/06/P06004
54. Steffen B, Seyfried A. Methods for measuring pedestrian density, flow, speed and direction with minimal scatter. *Physica A: Stat Mech Appl*. 2010;389(9):1902-1910. https://doi.org/10.1016/j.physa.2009.12.015
55. Liu X, Song W, Zhang J. Extraction and quantitative analysis of microscopic evacuation characteristics based on digital image processing. *Physica A: Stat Mech Appl*. 2009;388(13):2717-2726. https://doi.org/10.1016/j.physa.2009.03.017
56. Zhang J. *Pedestrian Fundamental Diagrams: Comparative Analysis of Experiments in Different Geometries: Zugl.: Wuppertal, Univ., Diss., 2012*, Schriften des Forschungszentrums Jülich IAS series, vol. 14. Jülich: Forschungszentrum Jülich; 2012.
57. Seyfried A, Passon O, Steffen B, Boltes M, Rupprecht T, Klingsch W. New insights into pedestrian flow through bottlenecks. *Trans Sci*. 2009;43(3):395-406. https://doi.org/10.1287/trsc.1090.0263
58. Seyfried A, Boltes M, Kähler J, et al. Enhanced empirical data for the fundamental diagram and the flow through bottlenecks. In: Klingsch W, Rogsch C, Schadschneider A, Schreckenberg M, eds. *Pedestrian and Evacuation Dynamics 2008*. Berlin and Heidelberg: Springer Berlin Heidelberg; 2010:145-156. https://doi.org/10.1007/978-3-642-04504-2_11
59. Seyfried A, Portz A, Schadschneider A. Phase coexistence in congested states of pedestrian dynamics. In: Bandini S, Manzoni S, Umeo H, Vizzari G, eds. *Cellular automata*, Lecture Notes in Computer Science. Berlin: Springer; 2010:496-505.
60. Boltes M, Zhang J, Seyfried A, Steffen B. T-junction: experiments, trajectory collection, and analysis. In: 2011 14th International IEEE Conference on Intelligent Transportation Systems. IEEE; 2011; Piscataway:158-165. https://doi.org/10.1109/ICCVW.2011.6130238
61. Zhang J, Klingsch W, Schadschneider A, Seyfried A. Ordering in bidirectional pedestrian flows and its influence on the fundamental diagram. *J Stat Mech Theory Exp*. 2012;2012(02):P02002. https://doi.org/10.1088/1742-5468/2012/02/P02002
62. Burghardt S, Seyfried A, Klingsch W. Performance of stairs—fundamental diagram and topographical measurements. *Trans Res Part C: Emerging Technol*. 2013;37:268-278. https://doi.org/10.1016/j.trc.2013.05.002
63. Liao W, Seyfried A, Zhang J, Boltes M, Zheng X, Zhao Y. Experimental Study on Pedestrian Flow through Wide Bottleneck. *Trans Res Procedia*. 2014;2:26-33. https://doi.org/10.1016/j.trpro.2014.09.005
64. Zhang J, Mehner W, Holl S, et al. Universal flow-density relation of single-file bicycle, pedestrian and car motion. *Phys Lett A*. 2014;378(44):3274-3277. https://doi.org/10.1016/j.physleta.2014.09.039

65. Bode N, Holl S, Mehner W, Seyfried A. Disentangling the impact of social groups on response times and movement dynamics in evacuations. *PloS one*. 2015;10(3):e0121227. https://doi.org/10.1371/journal.CongestionDynamicspone.0121227
66. Ziemer V, Seyfried A, Schadschneider A. Congestion dynamics in pedestrian single-file motion. In: Knoop V, Daamen W, eds. *Traffic and Granular Flow '15*, Vol. 12: Springer-Verlag New York Inc; 2016:89-96. https://doi.org/10.1007/978-3-319-33482-0_12
67. von Krüchten C., Müller F., Svachy A, Wohak oliver, Schadschneider A. Empirical study of the influence of social groups in evacuation scenarios. In: Knoop V, Daamen W, eds. *Traffic and Granular Flow '15*: Springer-Verlag New York Inc; 2016:65-72. https://doi.org/10.1007/978-3-319-33482-0_9
68. Cao S, Seyfried A, Zhang J, Holl S, Song W. Fundamental diagrams for multidirectional pedestrian flows. *J Stat Mech: Theory Exp*. 2017;3:033404. https://doi.org/10.1088/1742-5468/aa620d
69. von Krüchten C, Schadschneider A. Empirical study on social groups in pedestrian evacuation dynamics. *Physica A: Stat Mech Appl*. 2017;475:129-141. https://doi.org/10.1016/j.physa.2017.02.004
70. Wang J, Weng W, Boltes M, Zhang J, Tordeux A, Ziemer V. Step styles of pedestrians at different densities. *J Stat Mech Theory Exp*. 2018;2018(2):023406. https://doi.org/10.1088/1742-5468/aaac57
71. Wang J, Boltes M, Seyfried A, Zhang J, Ziemer V, Weng W. Linking pedestrian flow characteristics with stepping locomotion. *Physica A: Stat Mech Appl*. 2018;500:106-120. https://doi.org/10.1016/j.physa.2018.02.021
72. Haghani M, Sarvi M, Shahhoseini Z, Boltes M. How simple hypothetical-choice experiments can be utilized to learn humans' navigational escape decisions in emergencies. *PloS one*. 2016;11(11):e0166908. https://doi.org/10.1371/journal.pone.0166908
73. Haghani M, Sarvi M. Stated and revealed exit choices of pedestrian crowd evacuees. *Transp Res B Methodol*. 2017;95:238-259. https://doi.org/10.1016/j.trb.2016.10.019
74. Haghani M, Sarvi M, Shahhoseini Z. When 'push' does not come to 'shove': revisiting 'faster is slower' in collective egress of human crowds. *Transp Res A Policy Pract*. 2019;122:51-69. https://doi.org/10.1016/j.tra.2019.02.007
75. Haghani M, Sarvi M. 'Herding' in direction choice-making during collective escape of crowds: how likely is it and what moderates it. *Safety Sci*. 2019;115:362-375. https://doi.org/10.1016/j.ssci.2019.02.034
76. Haghani M, Sarvi M, Shahhoseini Z, Boltes M. Dynamics of social groups' decision-making in evacuations. *Transp Res C Emerging Technol*. 2019;104:135-157. https://doi.org/10.1016/j.trc.2019.04.029
77. Haghani M, Sarvi M. Simulating dynamics of adaptive exit-choice changing in crowd evacuations: model implementation and behavioural interpretations. *Transp. Res. C: Emerging Technologies*. 2019;103:56-82. https://doi.org/10.1016/j.trc.2019.04.009
78. Feliciani C, Nishinari K. Measurement of congestion and intrinsic risk in pedestrian crowds. *Transp. Res. C Emerging Technol*. 2018;91:124-155. https://doi.org/10.1016/j.trc.2018.03.027
79. Feliciani C, Murakami H, Nishinari K. A universal function for capacity of bidirectional pedestrian streams: filling the gaps in the literature. *PloS one*. 2018;13(12):e0208496. https://doi.org/10.1371/journal.pone.0208496
80. Fujita A, Feliciani C, Yanagisawa D, Nishinari K. Traffic flow in a crowd of pedestrians walking at different speeds. *Phys rev. E*. 2019;99(6). https://doi.org/10.1103/PhysRevE.99.062307
81. Subaih R, Maree M, Chraibi M, Awad S, Zanoon T. Gender-based insights into the fundamental diagram of pedestrian dynamics. In: Nguyen NT, Chbeir R, Exposito E, Aniorté P, Trawiński B, eds. *Computational Collective Intelligence*, Lecture Notes in Computer Science, vol. 11683. S.l.: Springer Nature; 2019:613-624. https://doi.org/10.1007/978-3-030-28377-3_51
82. Huang S, Wei R, Lo S, et al. Experimental study on one-dimensional movement of luggage-laden pedestrian. *Physica A: Stat Mech Appl*. 2019;516:520-528. https://doi.org/10.1016/j.physa.2018.09.038
83. Zhang J, Cao S, Salden D, Ma J. Homogeneity and activeness of crowd on aged pedestrian dynamics. *Procedia Comput Sci*. 2016;83:361-368. https://doi.org/10.1016/j.procs.2016.04.137
84. Kühne RD, ed.. *Hinweise zum Fundamentaldiagramm: Grundlagen und Anwendungen*. Ausg. 2005, FGSV, vol. 385. Köln: FGSV-Verl.; 2005.
85. Bosina E. *A New Generic Approach to the Pedestrian Fundamental Diagram*: ETH Zurich; 2018. https://doi.org/10.3929/ethz-b-000296226
86. Coifman B. Revisiting the empirical fundamental relationship. *Transp Res B Methodol*. 2014;68:173-184. https://doi.org/10.1016/j.trb.2014.06.005
87. Zhang J, Seyfried A. Comparison of intersecting pedestrian flows based on experiments. *Physica A: Stat Mech Appl*. 2014;405:316-325. https://doi.org/10.1016/j.physa.2014.03.004
88. Zhang J, Tordeux A, Seyfried A. Effects of boundary conditions on single-file pedestrian flow. In: Was Jaroslaw, ed. *Cellular automata*, Lecture Notes in Computer Science, vol. 8751. Cham: Springer; 2014:462-469. https://doi.org/10.1007/978-3-319-11520-7_48
89. Zhang J, Seyfried A. Quantification of bottleneck effects for different types of facilities. *Transp Res Procedia*. 2014;2:51-59. https://doi.org/10.1016/j.trpro.2014.09.008
90. Holl S. Methoden für die Bemessung der Leistungsfähigkeit multidirektional genutzter Fußverkehrsanlagen. *Dissertation*. Wuppertal; 2016.
91. Seyfried A, Steffen B, Klingsch W, Boltes M. The fundamental diagram of pedestrian movement revisited. *J Stat Mech Theory Exp*. 2005;2005(10):P10002. https://doi.org/10.1088/1742-5468/2005/10/P10002
92. Boltes M. *Automatische Erfassung präziser Trajektorien in Personenströmen hoher Dichte: Zugl.: Köln, Univ., Diss., 2014*, Schriften des Forschungszentrums Jülich IAS series, vol. 27. Jülich: Forschungszentrum Jülich Zentralbibl; 2015.

SUPPORTING INFORMATION

Additional supporting information may be found online in the Supporting Information section at the end of the article.

How to cite this article: Geoerg P, Schumann J, Holl S, Boltes M, Hofmann A. The influence of individual impairments in crowd dynamics. *Fire and Materials*. 2021;45:529–542. https://doi.org/10.1002/fam.2789

APPENDIX A: SUPPLEMENTARY MATERIAL 1 – ADDITIONAL EMPIRICAL RELATIONS

APPENDIX B: SUPPLEMENTARY MATERIAL 2 – PRECISION OF TRAJECTORIES

To extract the trajectories of each individual participant, the recordings of three camera perspectives were used (Figure 1). All cameras were mounted perpendicular in a height of 6.34 m above ground floor. The recordings had a minimum resolution of 1920 x 1080 pixel and a framerate of 25 s^{-1}. Assuming a participants maximum movement speed of 2 ms^{-1} leads to a spatial movement of 0.08 m.

The use of wide-angle cameras makes the consideration of image distortion necessary. Transferring the coordinate system of the real world to the coordinate system of the image was done by optimisation of reference points and the projected image points. The approach is described in detail in previous studies[50,51,92] and in Haghani et al.[72, Supporting Information 2]

Participants were asked to wear coloured caps according to their individual body height to increase the tracking quality of the individual position. The unique colour-coded pixel area were approximated by an ellipse, which the centre represents the position of a participant. This assumed position is shifted according to the inclination of the view. The error estimation of a participant's position consists of maximum detection error (e_{max}), systematic error caused by insufficient calibration (e_c), systematic error caused by coloured cap markers (e_m), and error variance of the position caused by wrong participant's height (e_h).[50, pp. 3] sqq

The maximal error (e_{max}) for the perspective of the 4k-camera was estimated by a linear combination (Equation B1) of the single errors due to calibration (e_c), marker detection (e_m) and body height (e_h).

$$e_{max} = e_c + e_m + e_h. \tag{B1}$$

Assuming a continuous detection and tracking of the heads, a sufficient auto-correction of the centred position of the head-ellipses and given that an error between two measuring points is less than or equal to a reference point, the maximum total error e_{max} at the edge of the 4k-perspective is as follows:

- 0.034 m for insufficient correction of the lens error.
- 0.058 m for not exact determination of participants body height.

Given Equation B1, the maximum error of a position in the 4k-perspective during the Bot_whe Bot_wal, and Bot_mix trials is 0,092 m ($e_{max} = 0.034\,m + 0,0\,m + 0,058\,m$) and during the Bot_ref trials 0,084 m ($e_{max} = 0.026\,m + 0,0\,m + 0,058\,m$). Here, the following assumptions were made:

e_{max}: should be negligible for reasonably conducted laboratory experiments.[51, p. 3]

e_c: 0,034 m for Bot_whe Bot_wal, and Bot_mix trials; 0.026 m for Bot_ref trials. The maximum calibration error was measured during the studies at head height on fixed reference points. It was calculated backwards by distance between real position and difference of pixels.

e_m: 0 , assuming a sufficient the auto-correction process of $\alpha \cdot 0.0012\,m$.

e_h: 0.058 m $\left(e_h = \frac{d_h}{2 \cdot tan(\alpha)}\right)$ with $d_h = 0.13\,m$ and $\alpha = 42°$.

Assuming a constant movement speed of a participant passing the entire camera perspective, the average error (e_{avg}) could be estimated by the following:

- 0.015 m for insufficient correction of the lens error, and
- 0.013 m for not exact determination of participants body height,

which results in an the average error (e_{avg}) of a position for the 4k-perspective of 0.028 m.